Analytical Methods

ROYAL SOCIETY OF CHEMISTRY

PAPER

View Article Online
View Journal

Check for updates

Cite this: DOI: 10.1039/d0ay00341g

Rapid and colorimetric detection of nucleic acids based on entropy-driven circuit and DNAzyme-mediated autocatalytic reactions†

Hongli Shi,[a] Jianyuan Dai, *[a] Fang Wang,[b] Yushun Xia,[a] Dan Xiao [ab] and Cuisong Zhou *[a]

In this work, a novel, rapid and enzyme-free colorimetric biosensor for the detection of nucleic acids has been developed based on entropy-driven (EDC) circuit and DNAzyme-mediated autocatalytic reactions. On sensing the target DNA, the EDC reaction could be initiated and the intact Mg^{2+}-dependent DNAzyme was formed in the reaction product; then, a "mimic target" DNA was generated during the cleavage process of DNAzyme, which in turn catalyzed the EDC reaction corresponding to an autocatalytic process. Meanwhile, numerous G-quadruplex structures were released and further interacted with hemin to form peroxidase-mimicking DNAzyme, inducing a remarkably amplified colorimetric signal. This autocatalytic EDC (AEDC) sensing system exhibited a linear relationship in the range from 20 pM to 10 nM with a detection limit of 10.2 pM. More importantly, benefitting from the Mg^{2+}-dependent DNAzyme-mediated autocatalytic reaction, the detection time (20 min) was significantly reduced compared to that for the reported EDC strategies. In addition, this sensing system has been applied for the detection of target DNA in human serum samples, indicating that it is promising for the on-site and real-time detection of nucleic acids in biomedical research and disease diagnosis.

Received 17th February 2020
Accepted 4th May 2020

DOI: 10.1039/d0ay00341g

rsc.li/methods

Published on 09 May 2020. Downloaded by Uppsala University on 5/26/2020 2:35:41 AM.

Introduction

The development of rapid and sensitive methods for the detection of nucleic acids is of great significance in biological studies, medical diagnosis, environmental monitoring and other fields.[1,2] The polymerase chain reaction (PCR) is the most widely used amplification technology for nucleic acid amplification and detection; however, it usually needs demanding conditions to maintain the activity of polymerase and also the existing complexity in the primer design.[3,4] To develop new methods to substitute the PCR technique, various signal amplification strategies, such as rolling circle amplification (RCA),[5,6] loop-mediated isothermal amplification (LAMP)[7,8] and strand displacement amplification (SDA),[9,10] have been applied for the sensitive detection of nucleic acids. However, these amplification strategies generally require auxiliary enzymes and complicated processes, which are both expensive and sensitive to reaction conditions. Therefore, the exploitation of simple, cost-effective and enzyme-free amplification schemes is urgent to ensure universal applications for nucleic acid detection. Recently, several toehold-aided DNA recycling amplifications such as the hybridization chain reaction (HCR),[11,12] catalytic hairpin assembly (CHA)[13,14] and entropy-driven catalytic (EDC) reaction[15,16] have been successfully used to achieve signal amplification for nucleic acid detection. These alternative DNA circuit systems that have the advantages of being enzyme-free (protein-free catalysts), convenience in usage and inexpensive exhibit steady signal output capacity and ease in building sensor platforms, which are increasingly applied for biological analysis. Among them, the CHA and HCR signal amplification methods driven by the free energy of base pair formation involve hairpin structures, which can cause difficulty in structural design and relatively high background and false-positive signals.[17–20] The entropy-driven catalytic (EDC) reaction as an alternative enzyme-free and hairpin-free amplification strategy can provide an applicable approach for clinical assays.[21–23] In the EDC system, target/trigger DNA catalyzed DNA circuit through toehold-mediated strand displacement reaction, and various single-stranded DNA molecules released into the system to play different roles within a network. Moreover, the total number of base pairs does not change before and after the reaction. Therefore, the EDC reaction is driven forward thermodynamically by the increase in entropy caused by the liberated molecules, which ensures the efficiency of the reaction process. Meanwhile, this catalytic mechanism has several benefits such as modularity, and flexibility of sequence design, which make it easy to build signal amplification platforms.[15,24–28] Tan's group developed a hairpin-free

[a]College of Chemistry, Sichuan University, Chengdu 610064, China. E-mail: daijy@scu.edu.cn; zcs@scu.edu.cn

[b]College of Chemical Engineering, Sichuan University, Chengdu 610065, China

† Electronic supplementary information (ESI) available. See DOI: 10.1039/d0ay00341g

Published on 09 May 2020. Downloaded by Uppsala University on 5/26/2020 2:35:41 AM.

amplification strategy for nucleic acid detection based on the EDC reaction, which exhibited excellent thermostability, high sensitivity and high selectivity. However, the time-consuming processes might limit the application of this method.[25] Thus, it is still a challenge to develop a rapid detection method based on the EDC amplification strategy. DNAzymes, screened through *in vitro* selection, are a class of catalytic nucleic acids with protease-like catalytic activities.[29,30] On account of simple synthetic preparation, good stability and high catalytic activity,[31,32] the metal ion-dependent DNAzymes have attracted considerable attention and have been applied for the detection of metal ions,[33] nucleic acids[34] and proteins.[35] Autocatalysis is a process based on exponential kinetics and can produce numerous replicas that are fed back into the system itself.[13,36] Recently, we designed a series of autocatalytic signal amplification systems using DNA self-replication, which significantly reduced the detection time.[14,37,38] Taking advantage of autocatalysis, we developed a rapid and colorimetric method for the detection of nucleic acids based on the EDC reaction and Mg^{2+}-dependent DNAzymes.

Experimental section

Materials and reagents

Hemin, 2,2′-azino-bis(3-ethylbenzothiazoline-6-sulfonic acid) ($ABTS^{2-}$), trishydroxymethylaminomethane acetic acid, magnesium chloride, potassium chloride and sodium hydroxide were purchased from Sigma-Aldrich (St. Louis, MO, USA). Ethylene diamine tetraacetic acid was obtained from Kelong (Chengdu, China). All other reagents were of analytical grade and were used without further purification. All oligonucleotide sequences were synthesized by Sangon Biotechnology Co. Ltd. (Shanghai, China) and purified by high-performance liquid chromatography (HPLC). The sequences of the oligonucleotides are given in Table S1.† Ultrapure water obtained from a Millipore water purification system (≥18.2 MΩ) was used in all experiments.

Instrumentation

Ultraviolet-visible light (UV-vis) measurements were performed with a U-2900 spectrophotometer (Hitachi Co. Ltd., Japan). The images of gel electrophoresis were scanned by the GenoSens 1800 Gel Image Analysis System (Clinx Science Instruments Co. Ltd., China).

Native polyacrylamide gel electrophoresis (PAGE)

First, 10 μL different reaction products with loading buffer were loaded into the lanes of the polyacrylamide gel (12%). The gel was run with 1× TBE buffer (45 mM Tris, 1.0 mM Na_2EDTA, pH 8.0) at a constant voltage of 100 V for 60 min at room temperature. The gel image was taken by the gel image analysis system after staining with ethidium bromide (EtBr) for 40 min.

Naked-eye observations and UV-vis biosensing assays

Complex Beacon and fuel strands (F) were heated to 95 °C for 5 min and then allowed to cool to room temperature for 3 h before the experiments. Then, different concentrations of target DNA were mixed with Beacon (500 nM), F (500 nM) and Hp (200 nM) in 100 μL TAE/Mg^{2+} buffer (40 mM tris-acetic acid, 1 mM EDTA, 12.5 mM magnesium chlorate, and 50 mM potassium chloride, pH 8.0) and then incubated for 20 min at room temperature to promote the EDC reaction. Subsequently, 2.5 μL of 50 μM hemin, 7.5 μL of 50 mM $ABTS^{2-}$, and 3 μL of 250 mM H_2O_2 were added into the abovementioned solution and incubated for another 10 min to proceed with the colorimetric reaction. The resulting solutions were then studied by naked-eye observations and UV-vis measurements, followed by absorbance measurements from 380 to 500 nm.

Results and discussion

Principle of AEDC amplification

We developed a rapid and colorimetric method for the sensitive detection of nucleic acids based on an autocatalysis-mediated EDC reaction. The strategy is depicted in Scheme 1 and comprises two parts: the upstream entropy-driven circuit and downstream Mg^{2+}-dependent DNAzyme-mediated autocatalytic reactions. Briefly, this system mainly consisted of a three-stranded DNA duplex complex (Beacon), a fuel strand (F) and a hairpin (Hp) as the substrate for DNAzyme. The sequence of Hp contains the hairpin loop that includes an adenine ribonucleotide (rA), which acts as the substrate for the Mg^{2+}-dependent DNAzyme. Moreover, the stem-loop structure region of Hp contains the sequence of the target DNA. Beacon was first prepared by annealing the mixture of R, P and Q strands. The sequence of the P strand contains the split G-quadruplex DNAzyme. The structure of Hp remains stable if the Mg^{2+}-dependent DNAzyme subunits are in an inactive configuration. In the presence of target DNA, it specifically attached to the recognition domain of Beacon, and the P strand was released; then, the released P strand folded quickly into a G-quadruplex. Meanwhile, the F strand bound to a newly exposed domain on the R–Q–T complex and formed a four-stranded complex R–F–Q–T. Finally, the R and T strands were released by the F strand from the four-stranded complex and a double-stranded complex F–Q was formed; then, the Mg^{2+}-dependent DNAzyme was constructed. The released T strand could trigger a new reaction cycle. Thus, the upstream circuit cycle driven forward by the

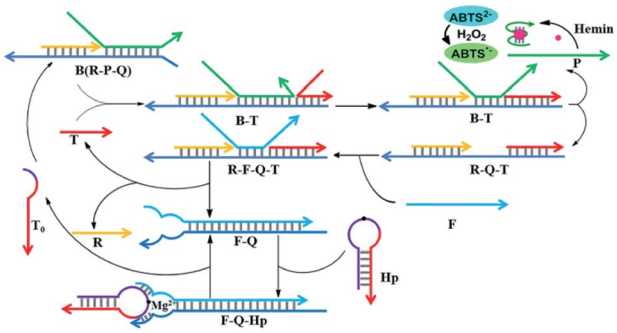

Scheme 1 Principle of the autocatalytic EDC (AEDC) reaction. Arrows drawn on DNA strands represent 3′ termini.

This journal is © The Royal Society of Chemistry 2020

Published on 09 May 2020. Downloaded by Uppsala University on 5/26/2020 2:35:41 AM.

increase in entropy was completed. For the downstream Mg^{2+}-dependent DNAzyme-mediated autocatalytic reaction, the formed Mg^{2+}-dependent DNAzyme could recognize and cyclically cleave toward its substrate Hp and produce a free single-stranded DNA trigger T_0. Since T_0 contained the same sequence of the target DNA, it was called as a "mimic target". Then, the produced "mimic target" could hybridize with the toehold of Beacon as the catalyst and trigger the AEDC reaction. As a result, a large number of G-quadruplex structures were produced. After interactions with hemin, the active hemin/G-quadruplex DNAzyme exhibited horseradish peroxidase (HRP)-mimicking activity and could effectively catalyze the H_2O_2-mediated oxidation of $ABTS^{2-}$ to green-colored $ABTS^{\bullet-}$, thus providing an amplified colorimetric signal, which could be easily read out with the naked eye. The circular use of target DNA and its "mimic target" in the AEDC reaction could quickly and prominently reduce the reaction time and generate a higher signal.

Feasibility of the amplification strategy

To verify the feasibility of this amplification strategy, the absorbance spectrum of the control group in the absence of Hp was also measured for comparison (Fig. 1A). After the addition of target DNA, both the absorbance signals increased. However, compared with the observation for the simple EDC reaction (curves a and b), an obvious signal enhancement could be observed due to the introduction of Hp (curves c and d). The maximum absorption value was obtained at 20 min. These results strongly indicate that this new signal amplification strategy is efficient for the amplified detection of target DNA. Evidently, this rapid signal amplification was achieved by the "mimic target", which was obtained by the catalytic cleavage of the Mg^{2+}-dependent DNAzyme toward its substrate. Furthermore, polyacrylamide gel electrophoresis (PAGE) analysis was also implemented to verify the feasibility of the AEDC reaction system. As shown in Fig. 1B, when Beacon and the F strand were applied, only a weak band of the F–Q complex was observed, which could be attributed to the intrinsic leakage reactions (lane 2). The weak bands of the F–Q complex and P strand (G-quadruplex DNAzyme sequence) could be observed with the addition of the target DNA (lane 4), indicating that the EDC reaction was triggered. In the presence of Hp, the color of the bands of the F–Q complex and P strand became darker (lane 6), indicating that the Mg^{2+}-dependent DNAzyme-mediated autocatalytic reaction truly occurred. These results were quite consistent with the absorbance spectral data.

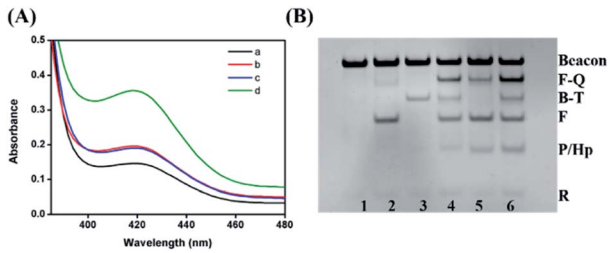

Fig. 1 Feasibility of the DNA detection strategy. (A) Absorbance spectra of solutions under different conditions ((a) Beacon + F, (b) Beacon + F + T, (c) Beacon + F + Hp, (d) Beacon + F + Hp + T). (B) Polyacrylamide gel electrophoresis images for the DNA detection system. Lane 1: Beacon; lane 2: Beacon + F; lane 3: Beacon + T, lane 4: Beacon + F + T; lane 5: Beacon + F + Hp; lane 6: Beacon + F + Hp + T. The final concentrations of Beacon, F and Hp were 500 nM, 500 nM and 200 nM, respectively. The concentration of target was 10 nM in the absorbance experiment and 50 nM in the gel electrophoresis experiment. All measurements were performed in Tris–Ac buffer solution (40 mM, 1 mM EDTA, 12.5 mM $MgCl_2$, 50 mM KCl, pH 8.0).

Optimization of the experimental conditions

In order to obtain the best sensing performance of this proposed strategy, several experimental conditions including the concentration ratio of Beacon to F, the concentration of Hp, and reaction time were optimized. The signal-to-noise ratio A_{pre}/A_{ab} (the absorbance intensity at 418 nm of the detection system in the presence of 10 nM target DNA *versus* the absorbance intensity at 418 nm of the detection system in the absence of target DNA) was used to evaluate the performance of this system. As shown in Fig. 2A and B, with the increase in the molar ratio of Beacon to F and the concentration of Hp, A_{pre}/A_{ab} reached the maximum value at 1 : 1 of Beacon/F and 200 nM Hp. With the further increase in the molar ratio of Beacon and the concentration of Hp, the A_{pre}/A_{ab} value decreased due to the enhancement in the background. The A_{pre}/A_{ab} value of the AEDC reaction system increased much faster than that of the

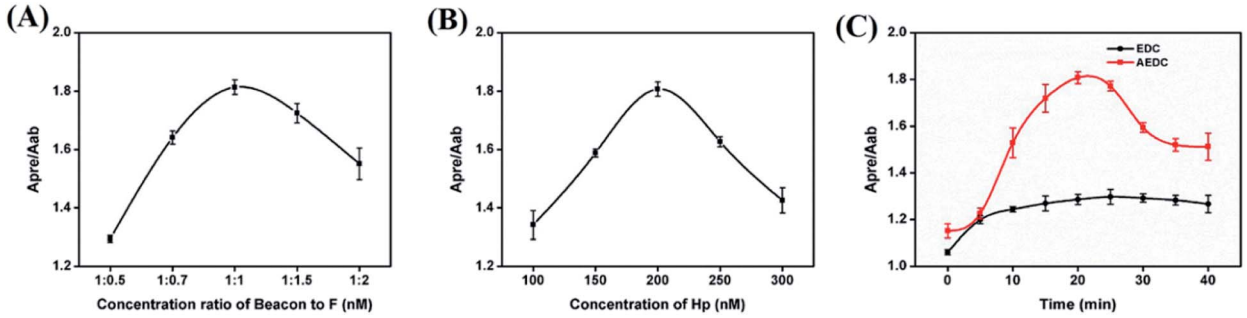

Fig. 2 Optimization of the reaction conditions for the efficient analysis of DNA: the concentration ratio of Beacon to F (A), the concentration of Hp (B), and reaction time (C). A_{pre}/A_{ab}: the absorbance intensity at 418 nm of the detection system in the presence of 10 nM target DNA *versus* the absorbance intensity at 418 nm of the detection system in the absence of target DNA.

Published on 09 May 2020. Downloaded by Uppsala University on 5/26/2020 2:35:41 AM.

system without Hp and reached maximum at around 20 min (Fig. 2C). Furthermore, the ratio of the absolute absorption intensity ($A_{AEDC} - AAEDC0$)/($A_{EDC} - AEDC0$) was used as another method to verify that the Mg^{2+}-dependent DNAzyme-mediated autocatalytic reaction significantly reduced the detection time; here, $AAEDC0$ and A_{AEDC} are the absorbance intensities of the AEDC system in the absence and presence of target DNA, respectively, and $AEDC0$ and A_{EDC} are the absorbance intensities of the EDC system in the absence and presence of target DNA, respectively. The ratio of the absolute absorbance intensity between the AEDC and EDC systems at 20 min was calculated to be around 3.0 (Fig. S1†). This rapid signal response could be attributed to the Mg^{2+}-dependent DNAzyme-mediated autocatalytic reaction. It should be noted that in the absence of target DNA, the background signal of the AEDC system increased with the increase in the reaction time, which could be ascribed to the uncatalyzed (leakage) reaction. This is a slight amount of leakage reaction when both the Beacon complex and fuel strand are present.[15,16,25,39] Therefore, in accordance with these results, the above-mentioned optimum experimental conditions were adopted for the subsequent experiments.

Analytical performance of the AEDC reaction strategy for DNA detection

Under the optimized experimental conditions, the detection performance of this proposed amplification strategy towards target DNA was investigated. As shown in Fig. 3, a series of samples containing different concentrations of target DNA have been tested. The image of sample solutions after the addition of target DNA with concentrations ranging from 0 to 10 nM is shown in Fig. 3A. From the image, we can see that the color transition is gradually intensified with the increase in the amount of the added target DNA. Furthermore, when the target DNA concentration was as low as 50 pM, an obvious color transition could be observed by the naked eye without using any complex instruments. Fig. 3B exhibits the UV-vis absorption spectra of the amplification system toward target DNA standards with different concentrations. With the addition of target DNA concentrations, the absorbance at 418 nm gradually increased. Accordingly, the absorbance intensity at 418 nm was employed to quantitatively scale the target DNA concentration. A curve was obtained between the absorption intensity and the concentration of target DNA from 20 pM to 10 nM (Fig. 3C). In the range from 20 pM to 500 pM of the target DNA concentration, we found an excellent linear correlation between the absorbance and the target DNA concentration at 418 nm (inset of Fig. 3C). The detection limit was calculated to be 10.2 pM based on the mean response of the blank tests ($n = 11$) plus 3 times the standard deviation (3σ), which was comparable to or better than those for previous colorimetric DNA detection systems. This proposed strategy needs a much shorter time (20 min) than that of previous assays, especially other EDC-based signal amplification assays (Table S2†).[40–46]

Specificity of the proposed amplification strategy for target DNA detection

To further investigate the selectivity of the detection system, the absorbance of four kinds of DNA sequences, namely, deleted, inserted, mismatched, and perfectly matched target DNA was tested under the same experimental conditions. The experimental results are shown in Fig. 4. We found that the perfectly matched target DNA could result in obviously increased absorbance, but the other three DNA sequences only showed lower absorbance. Importantly, this selectivity could be visualized

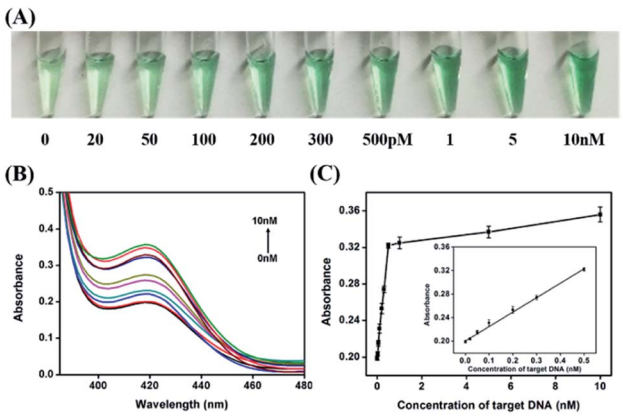

Fig. 3 (A) Photograph of the colorimetric detection system in the presence of target DNA at different concentrations. Concentrations of Beacon, F and Hp: 500 nM, 500 nM and 200 nM. (B) Absorption spectra corresponding to the analysis of target DNA at different concentrations (from bottom to top: 0 pM, 20 pM, 50 pM, 100 pM, 200 pM, 300 pM and 500 pM and 1 nM, 5 nM and 10 nM). (C) Relationship between the intensity change in absorbance and target DNA concentrations. Inset shows the linear relations between the absorption intensity and the concentrations of target DNA from 20 to 500 pM. The error bars represent the standard deviations of three parallel tests.

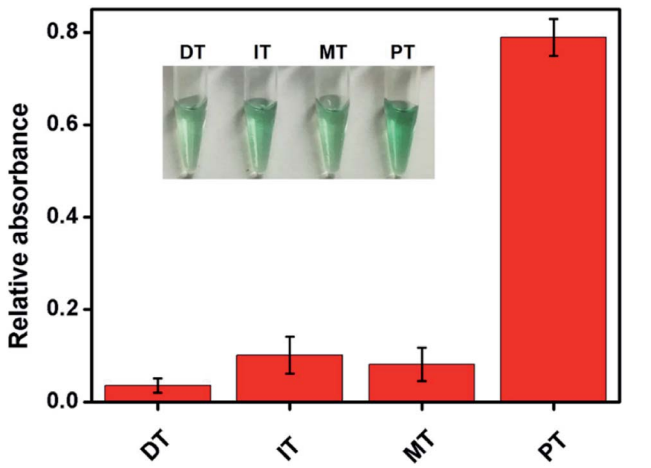

Fig. 4 Specificity of this strategy for target DNA detection. Histogram of absorbance signals for deleted target (DT), inserted target (IT), mismatched target (MT) and perfectly matched target (PT). The concentrations of Beacon, F and Hp were 500 nM, 500 nM and 200 nM, respectively; MT, DT, IT, and PT: 10 nM. Inset: Photographs of the reaction solutions in the presence of various target DNA strands. The error bars represent the standard deviations of three parallel tests.

This journal is © The Royal Society of Chemistry 2020

Published on 09 May 2020. Downloaded by Uppsala University on 5/26/2020 2:35:41 AM.

Table 1 Recovery analysis of target DNA in human serum samples

Sample	Added (pM)	Detected (pM) ($n = 3$)	Recovery (%)	RSD (%) ($n = 3$)
1	200	197.6	98.8	3.1
2	300	310.3	103.4	4.6
3	400	376.9	94.2	3.3

with the naked eye. This result demonstrates that the detection system is highly selective toward its completely complementary DNA. This can be ascribed to the fact that only the target DNA can trigger the AEDC reaction process to generate abundant G-quadruplex DNAzymes for the signal output.

Detection of target DNA in human serum samples

To investigate the practicality of the proposed strategy for DNA detection in real biological samples, three samples containing 200 pM, 300 pM and 400 pM target DNA were added to 100-fold-diluted human real serum samples. The results are listed in Table 1. The recovery of target DNA ranged from 94.2 to 103.4% and the RSDs ranged from 3.1 to 4.6%, which suggested that the AEDC strategy could become a practical tool for DNA assays in real biological samples.

Conclusions

In summary, we have successfully developed a rapid, enzyme-free and colorimetric sensing system for the sensitive detection of nucleic acids based on entropy-driven circuit and DNAzyme-mediated autocatalytic reactions. Compared with previously reported methods, the sensing system demonstrated considerable advantages, such as being enzyme-free and label-free and a shorter reaction time. The novel detection system could be sensitively identified with the naked eye. In addition, due to the flexibility of the sequence design, we only need to modify the recognition domains of the sensing system to detect various analytes. Therefore, we believe that the proposed strategy holds great potential in practical applications and future point-of-care clinical diagnosis.

Conflicts of interest

There are no conflicts to declare.

Acknowledgements

This work was financially supported by the National Natural Science Foundation of China (No. 21777108 and 21775106).

References

1 J. Huang, Y. R. Wu, Y. Chen, Z. Zhu, X. H. Yang, C. Y. J. Yang, K. Wang and W. H. Tan, *Angew. Chem., Int. Ed.*, 2011, **50**, 401–404.
2 S. Bi, J. L. Zhang and S. S. Zhang, *Chem. Commun.*, 2010, **46**, 5509–5511.
3 R. K. Saiki, D. H. Gelfand, S. Stoffel, S. J. Scharf, R. Higuchi, G. T. Horn, K. B. Mullis and H. A. Erlich, *Science*, 1988, **239**, 487–491.
4 C. Chen, D. A. Ridzon, A. J. Broomer, Z. Zhou, D. H. Lee, J. T. Nguyen, M. Barbisin, N. L. Xu, V. R. Mahuvakar and M. R. Andersen, *Nucleic Acids Res.*, 2005, **33**, E179.
5 P. M. Lizardi, X. H. Huang, Z. R. Zhu, P. Bray-Ward, D. C. Thomas and D. C. Ward, *Nat. Genet.*, 1998, **19**, 225–232.
6 H. Y. Liu, L. Li, L. L. Duan, X. Wang, Y. X. Xie, L. L. Tong, Q. Wang and B. Tang, *Anal. Chem.*, 2013, **85**, 7941–7947.
7 T. Notomi, H. Okayama, H. Masubuchi, T. Yonekawa, K. Watanabe, N. Amino and T. Hase, *Nucleic Acids Res.*, 2000, **28**, E63.
8 B. L. Li, X. Chen and A. D. Ellington, *Anal. Chem.*, 2012, **84**, 8371–8377.
9 D. Y. Zhang and E. Winfree, *J. Am. Chem. Soc.*, 2009, **131**, 17303–17314.
10 Z. Y. Fang, W. Wu, X. W. Lu and L. W. Zeng, *Biosens. Bioelectron.*, 2014, **56**, 192–197.
11 R. M. Dirks and N. A. Pierce, *Proc. Natl. Acad. Sci. U. S. A.*, 2004, **101**, 15275–15278.
12 Y. Chen, J. Xu, J. Su, Y. Xiang, R. Yuan and Y. Q. Chai, *Anal. Chem.*, 2012, **84**, 7750–7755.
13 P. Yin, H. M. T. Choi, C. R. Calvert and N. A. Pierce, *Nature*, 2008, **451**, 318–323.
14 J. Y. Dai, H. F. He, Z. J. Duan, Y. Guo and D. Xiao, *Anal. Chem.*, 2017, **89**, 11971–11975.
15 D. Y. Zhang, A. J. Turberfield, B. Yurke and E. Winfree, *Science*, 2007, **318**, 1121–1124.
16 D. Y. Zhang, R. F. Hariadi, H. M. T. Choi and E. Winfree, *Nat. Commun.*, 2013, **4**, 1965–1974.
17 Y. Qian, C. Y. Wang and F. L. Gao, *Biosens. Bioelectron.*, 2015, **63**, 425–431.
18 G. Seelig, B. Yurke and E. Winfree, *J. Am. Chem. Soc.*, 2006, **128**, 12211–12220.
19 Y. Jiang, B. L. Li, J. N. Milligan, S. Bhadra and A. D. Ellington, *J. Am. Chem. Soc.*, 2013, **135**, 7430–7433.
20 F. Xuan and I. M. Hsing, *J. Am. Chem. Soc.*, 2014, **136**, 9810–9813.
21 Y. J. Li, X. J. Ding, D. D. Li, H. P. Wu, W. Huang and S. J. Ding, *Anal. Methods*, 2019, **11**, 1613–1619.
22 X. L. Zhang, Z. H. Yang, Y. Y. Chang, D. Liu, Y. R. Li, Y. Q. Chai, Y. Zhuo and R. Yuan, *Chem. Sci.*, 2020, **11**, 148–153.
23 W. Diao, M. Tang, S. J. Ding, X. M. Li, W. B. Cheng, F. Mo, X. Y. Yan, H. M. Ma and Y. R. Yan, *Biosens. Bioelectron.*, 2018, **100**, 228–234.
24 S. Bi, J. L. Zhang, S. Y. Hao, C. F. Ding and S. S. Zhang, *Anal. Chem.*, 2011, **83**, 3696–3702.
25 Y. F. Lv, L. Cui, R. Z. Peng, Z. L. Zhao, L. P. Qiu, H. P. Chen, C. Jin, X. B. Zhang and W. H. Tan, *Anal. Chem.*, 2015, **87**, 11714–11720.
26 S. Ou, T. Xu, X. Liu, X. Y. Yu, R. Li, J. Deng, J. X. Yuan and Y. M. Chen, *Sens. Actuators, B*, 2018, **255**, 3057–3063.
27 C. Zhang, Z. Y. Wang, Y. Liu, J. Yang, X. X. Zhang, Y. F. Li, L. Q. Pan, Y. G. Ke and H. Yan, *J. Am. Chem. Soc.*, 2019, **141**, 17189–17197.

Published on 09 May 2020. Downloaded by Uppsala University on 5/26/2020 2:35:41 AM.

28 E. H. Xiong, D. S. Zhen and L. Jiang, *Chem. Commun.*, 2018, **54**, 12594–12597.
29 J. W. Liu, Z. H. Cao and Y. Lu, *Chem. Rev.*, 2009, **109**, 1948–1998.
30 I. Willner, B. Shlyahovsky, M. Zayats and B. Willner, *Chem. Soc. Rev.*, 2008, **37**, 1153–1165.
31 J. Yang, R. F. Wu, Y. F. Li, Z. Y. Wang, L. Q. Pan, Q. Zhang, Z. H. Lu and C. Zhang, *Nucleic Acids Res.*, 2018, **46**, 8532–8541.
32 H. S. Yin, B. C. Li, Y. L. Zhou, H. Y. Wang, M. H. Wang and S. Y. Ai, *Biosens. Bioelectron.*, 2017, **96**, 106–112.
33 J. Elbaz, B. Shlyahovsky and I. Willner, *Chem. Commun.*, 2008, **13**, 1569–1571.
34 Y. H. Wan, Y. J. Zhou, K. J. Xiao, C. P. Nie, J. Zhang, C. Liu, T. T. Chen and X. Chu, *Chem. Commun.*, 2019, **55**, 3278–3281.
35 J. M. Yang, B. T. Dou, R. Yuan and Y. Xiang, *Anal. Chem.*, 2016, **88**, 8218–8223.
36 F. Wang, J. Elbaz, C. Teller and I. Willner, *Angew. Chem., Int. Ed.*, 2011, **50**, 295–299.
37 H. F. He, J. Y. Dai, G. X. Dong, H. L. Shi, F. Wang, Y. R. Qiu, R. X. Liao, C. S. Zhou, Y. Guo and D. Xiao, *Anal. Chem.*, 2019, **91**, 3043–3047.
38 G. X. Dong, J. Y. Dai, L. M. Jin, H. L. Shi, F. Wang, C. S. Zhou, B. Z. Zheng, Y. Guo and D. Xiao, *Anal. Methods*, 2019, **11**, 2537–2541.
39 X. P. Olson, S. Kotani, J. E. Padilla, Na. Hallstrom, S. Goltry, J. Lee, B. Yurke, W. L. Hughes and E. Graugnard, *ACS Synth. Biol.*, 2017, **6**, 84–93.
40 P. Liu, X. H. Yang, S. Sun, Q. Wang, K. M. Wang, J. Huang, J. B. Liu and L. L. He, *Anal. Chem.*, 2013, **85**, 7689–7695.
41 J. Dong, X. Cui, Y. Deng and Z. Tang, *Biosens. Bioelectron.*, 2012, **38**, 258–263.
42 F. Xuan, X. T. Luo and I. M. Hsing, *Anal. Chem.*, 2012, **84**, 5216–5220.
43 H. Y. Zhao, L. Wang, J. Zhu, H. P. Wei and W. Jiang, *Talanta*, 2015, **138**, 163–168.
44 B. Wang, X. Zhou, D. B. Yao, X. B. Sun, M. He, X. J. Wang, X. Yin and H. J. Liang, *Chem. Commun.*, 2017, **53**, 10950–10953.
45 Z. J. Duan, Z. Li, J. Y. Dai, H. F. He and D. Xiao, *Talanta*, 2017, **164**, 34–38.
46 H. L. Li, J. T. Ren, Y. Q. Liu and E. K. Wang, *Chem. Commun.*, 2014, **50**, 704–706.

 This journal is © The Royal Society of Chemistry 2020